Third Astrophysics Conference
Proceedings–"The Cosmic
Background Radiation and
Fundamental Physics"
Rome, Italy 1984

OBSERVATIONS OF THE LARGE SCALE ANISOTROPY IN THE COSMIC BACKGROUND RADIATION AT 3 mm

Philip M. Lubin and Thyrso Villela Neto †

Space Sciences Laboratory and Lawrence Berkeley Laboratory
University of California, Berkeley, CA 94720, USA
† and Instituto de Pesquisas Espaciais - INPE/CNPq
Departamento de Astrofísica
12200 - São José dos Campos, SP, Brazil

Summary. - We present data from a series of balloon flights in both hemispheres to measure the large scale anisotropy at 3 mm wavelength. The data cover 85% of the sky to a sensitivity of 0.7 mK per 7° field of view. The instrument is sufficiently sensitive to resolve the dipole in real-time as the gondola rotates. The motion of the earth around the sun has been seen in flights separated by 6 months. A 90% confidence level upper limit of 7×10^{-5} is obtained for a quadrupole component. Galactic contamination is very small with less than 0.1 mK contribution to the dipole and quadrupole. When compared to other dipole measurements at different wavelengths, the data can be useful in determining the temperature or deviation from blackbody of the radiation.

1. - INTRODUCTION

Isotropy and homogeneity on large scales are fundamental in our description of the universe. Because of the simplicity of these assumptions and the solvable nature of the equations which arise from this, isotropy and homogeneity continue to dominate cosmological theory. Experimentally these appear to be very poor descriptions, at least in the visible portion of the spectrum where clustering of galaxies, voids and other inhomogeneities are seen. For the cosmic background radiation (CBR) however, isotropy and homogeneity are perfectly consistent with the data, though very little is known about the latter, except from CN measurements which do not really test homogeneity at cosmological distances. The fact that from scales of the order of arc seconds to a hundred degrees no intrinsic anisotropy has been found in twenty years leaves us with a very simple but puzzling picture.

As experiments have advanced in sensitivity, new ideas, such as the inflationary universe models, have been invoked to explain the lack of observable anisotropies. Measurements of isotropy on small scales are now putting limits on the order of 10^{-5} on intrinsic variations (Uson and Wilkinson 1984). Already theorists are straining to explain the current limits. On large angular scales ($>10°$), near full sky ($>80\%$) maps are now available at 3, 8, and 12 mm wavelength with current quadrupole limits of 7×10^{-5} (90% C.L.). However, we are beginning to have trouble from a local source of interference, namely, our galaxy. By judicious choice of frequencies and modeling of galactic emission further improvement is possible, but more than another order of magnitude will be extremely difficult at the largest scales (quadrupole).

2. - EXPERIMENT MOTIVATION

We began an experiment in 1980 to measure the large scale anisotropy at 3.3 mm wavelength. The original motivation for this wavelength was to test for the effect of a possible spectral distortion, seen near the peak of the spectrum (Woody and Richards 1979), on the dipole. In addition, the experiment proved to be useful in placing limits on higher order anisotropies. Low noise cryogenic millimeter wave coherent receivers were showing great promise, so a 3.3 mm (90 GHz) liquid-helium-cooled Mott diode receiver was used, based on a mixer design by Kerr (Cong, Kerr and Mattauch 1979).

3. - SPECTRAL DETERMINATION

Assuming that the dipole anisotropy is due to our motion relative to the radiation, the dipole amplitude will depend on wavelength in a manner characteristic of the spectrum of the radiation. This effect can be used to determine the spectrum of the radiation from the measured dipole as a function of wavelength (Lubin 1980,1982; Danese and De Zotti 1981). If the radiation has a blackbody spectrum, two dipole measurements, in theory, will determine the temperature. Spectral distortions can be similarly measured, particularly if the spectral index (derivative) is large or a strong function of wavelength.

Consider an isotropic radiation field, not necessarily blackbody, of intensity $I(ergs\ cm^{-2}\ \mathrm{sec}^{-1}\ st^{-1}\ Hz^{-1})$. In a reference frame moving with velocity β the intensity I' will be:

$$I' = I\left(\frac{\nu'}{\nu}\right)^3 \qquad with \qquad \nu' = \gamma\nu\left(1 + \beta\cos\theta\right) ,$$

where θ is the angle of observation. This transformation follows immediately from the Lorentz invariance of the phase space density. For a blackbody this gives the familiar result that the radiation field in the moving frame is also blackbody but with an angle dependent temperature leaving T/ν invariant. For an isotropic power law distribution $I \sim \nu^{\alpha}$ and for small β the transformed field is :

$$I'(\theta') = I_0'\,(1 + (3 - \alpha)\beta\cos\theta) .$$

Compton and Getting (1935) derived a similar result for the velocity dependent distribution of cosmic rays. For $\alpha = 3$ there is no anisotropy, since the spectrum changes with frequency in the same manner as the relativistic contraction of solid angle ($\sim \nu^2$) and the change in photon energy ($\sim \nu$). For $\alpha > 3$ the maximum flux is in the backward ($\theta = 180^\circ$) direction contrary to intuition. For a Planck (blackbody) spectrum α is always less than 2, being 2 in the low frequency limit and becoming increasingly negative at high frequencies.

It is convenient to express the flux as a temperature, so an "antenna temperature" $T_A \equiv \frac{\lambda^2}{2k} I$ is defined as the equivalent physical temperature of a blackbody which gives the flux I in the low frequency (Rayleigh-Jeans) limit. The motion induced anisotropy is then:

$$T_A(\theta) = T_{A_0}(1 + (3 - \alpha)\beta\cos\theta) \quad \text{for} \quad \left|3 - \alpha\right| \beta \ll 1 .$$

The amplitude of the anisotropy is then $\Delta T_A / T_A = (3 - \alpha)\beta\cos\theta$ with ΔT_A being the quantity directly measured in anisotropy experiments. The anisotropy magnitude depends on the intensity, spectral index (derivative) and velocity. For a blackbody, the spectral index and flux are uniquely related to the temperature

and frequency, so two dipole measurements at different frequencies determine both the temperature of the radiation and our velocity through it. The uncertainty in temperature determined is:

$$\frac{\sigma_T}{T} \sim 2.8 \left(\left(\frac{\sigma_{\Delta T_A}}{\Delta T_A} \right)^2_{12mm} + \left(\frac{\sigma_{\Delta T_A}}{\Delta T_A} \right)^2_{3mm} \right)^{1/2},$$

if we use, for example, two measurements at 3 mm and 12 mm of a blackbody with temperature near 3 K. The best dipole measurements to date have an accuracy of about 5% limited by calibration errors, though a 1 - 2% measurement is possible from a satellite or a balloon if a suitable calibrator is used. A 1% anisotropy measurement at 3 mm and 12 mm would give $\sigma_T \sim 0.1$ K, the current 5% uncertainty gives $\sigma_T \sim 0.5$ K. The relative accuracy increases with anisotropy measurements above the peak of the spectrum where α, and therefore the dipole, is a strong function of the temperature of the radiation. Here, even a modest dipole measurement (5-10%) could yield significant information about the spectrum at submillimeter wavelengths. There are more direct ways of measuring the spectrum, but this is a side benefit of anisotropy measurements and is an important cross check. These arguments can also be used for some types of higher order distortions and polarizations as well as for cluster cooling effects.

One area where this comparison is useful is where there is any spectral distortion or rapid change in slope. The dipole is very sensitive to changes in slope as it essentially measures the product of the flux and its first derivative. The spectrum measurements of Woody and Richards provides one area of test as does the recent two component massive photon theory of Georgi, Ginsparg and Glashow (Georgi *et al.* 1983; de Bernardis *et al.* 1984) invoked to explain the Woody and Richards data. A precise prediction of the dipole expected from the Woody and Richards data is not possible because of the flux uncertainty and spectral resolution of their data. However, fitting a smooth spectrum through their data yields an estimated 20% to 40% enhancement of the dipole at our wavelength over that expected from a 2.7 K blackbody (Lubin 1982).

4. - EXPERIMENT DESCRIPTION

The radiometer and gondola used is shown in Figure 1. It is a Dicke radiometer which uses a rotating mirror to chop between two positions in the sky 90° apart. The difference in temperature between two positions in the sky is measured as the apparatus rotates. The rotation of the gondola and the earth gives a sky coverage of about 30% per flight. The gondola typically hangs 70 m below a 3×10^4 m^3 balloon and rotates at 0.5 revolutions per minute. The typical flight altitude is 30 Km with a 10 mb residual atmosphere for a duration of 10 to 15 hours. The instrument is calibrated inflight with a blackbody target whose temperature is measured. Two sets of magnetometers, fluxgate and Hall effect, provide the orientation of the package relative to the earth's magnetic field.

The microwave radiometer used is shown in Figure 2. The instrument is described in detail in Epstein (1983). It consists of a low-doped GaAs Schottky diode mixer operated at 4.2 K (liquid helium) and pumped by a 90 GHz Gunn effect oscillator. The mixer has a conversion loss of about 6 dB. After the signal is downconverted, it is amplified by a 2 stage GaAs FET IF amplifier, also cooled to 4.2 K. The IF amplifier has a noise temperature of about 20 K and a gain of 24 dB over a 600 MHz bandwidth centered at 1.4 GHz. The antenna is a 7° FWHM corrugated scalar feedhorn operated at 77 K. The radiation is coupled

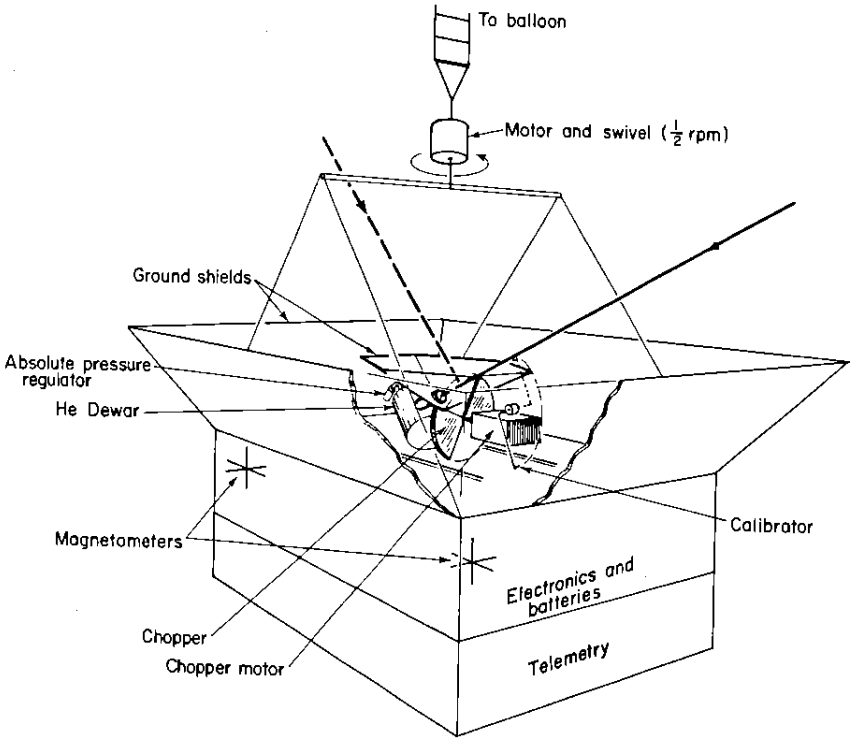

Fig. 1. - Gondola and instrumentation.

into the dewar through a 130 μ mylar window. The pressure of the liquid helium and liquid nitrogen is controlled by absolute pressure regulators.

The beam is chopped by a highly polished rotating aluminum mirror, phase locked to a crystal to chop at 23 2/3 Hz. The mirror introduces an offset of 200 mK due to its emissivity of about 8 x 10^{-4}. The offset drift was typically 1 mK per hour. The signal is blanked as the edge of the mirror crosses the beam with a 20 % blanking time to prevent beam scattering as the mirror crosses the antenna. The chopped signal is demodulated by a synchronous detector and recorded on tape as well as telemetered to the ground.

The system has an equivalent noise temperature of 130 K, double side band, averaged over the 500 MHz equivalent bandwidth (corrected for gain variations). A square-wave switched square-wave demodulated radiometer with noise temperature T_s, bandwidth B, frequency ν and integration time τ has an equivalent temperature fluctuation of:

$$\Delta T = \frac{\sinh x/2}{x/2} \frac{2T_s}{\sqrt{B\tau}} \sim \frac{2T_s}{\sqrt{B\tau}} \quad with \quad x = \frac{h\nu}{kT} .$$

Using the measured system parameters above gives $\Delta T = 12$ mK/Hz$^{1/2}$. Increasing this by 10% because of the 20% beam blanking time gives 13 mK/Hz$^{1/2}$. The measured inflight ΔT is 14.0 $\pm$ 0.1 mK/Hz$^{1/2}$, in relatively good agreement. In one rotation of the gondola ($\tau \sim 100$ seconds) the equivalent fluctuation is about 1 mK, so the dipole ($\sim$3 mK) should be observable in real time as the instrument rotates. As can be seen in Figure 3 of a telemetry strip chart from the April 1982 flight with a 55s RC filter in line, the dipole is readily observed.

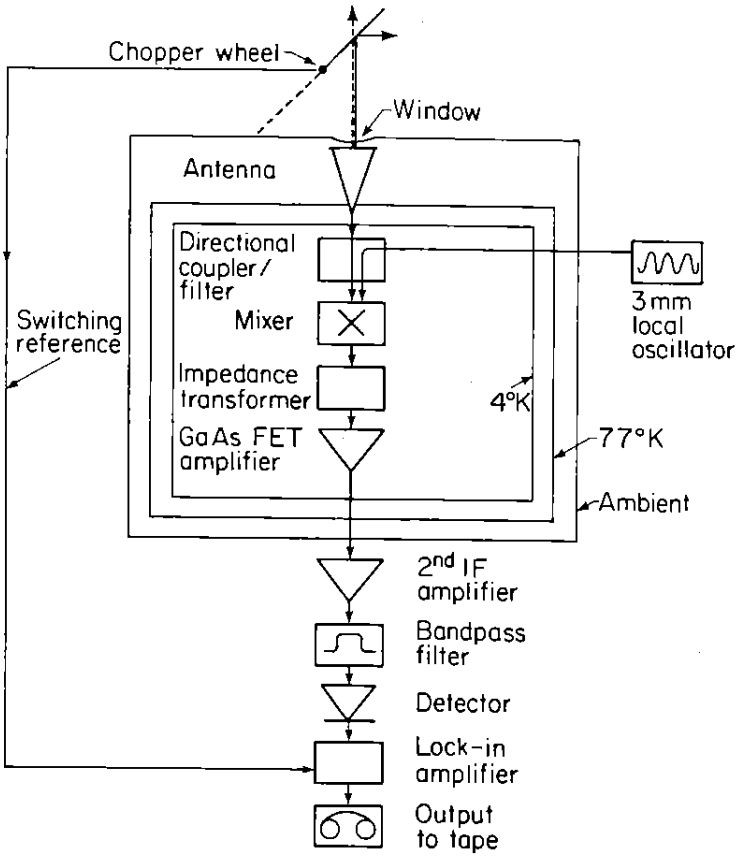

Fig. 2. - Schematic of 3.3 mm radiometer.

5. - ATMOSPHERIC EMISSION

Because of the minute nature of the signals being measured, atmospheric emission requires attention and dictates the frequency ranges useful for observation and the altitudes required. Figure 4 shows the calculated vertical atmospheric emission at 30 Km altitude based on the oxygen, water and ozone line strengths and concentrations, and the atmospheric temperature profile. Above 95 GHz numerous ozone lines are present along with oxygen and water lines. Below 95 GHz the primary lines are the set of oxygen lines near 60 GHz and a water line at 22 GHz. At our center frequency of 90.0 GHz and bandpass of 88.3 to 91.7 GHz, the total calculated vertical atmospheric emission is 6 mK at our float altitude of 30 Km. As can be seen from Figure 4 we are in a broad minimum of ozone and oxygen emission. Most of the water is frozen out with a residual precipitable water column of 0.3 μ. Figure 5 shows the calculated emission at 90 GHz as a function of altitude.

To first order, because the beam directions are symmetrical about the zenith $\pm$ 45°, atmospheric emission cancels out, since we only measure the temperature difference. In reality, due to wind shears, the gondola wobbles slightly, with an amplitude measured to be less than 1/3°. This yields an atmospheric signal of less than 0.1 mK. As this is already at such a low level and is in general not synchronized on the sky, no correction is necessary. Patchy atmospheric emission is a potential problem and some evidence is seen for this in submillimeter measurements, though scaling to our atmospheric emission level indicates that it is not

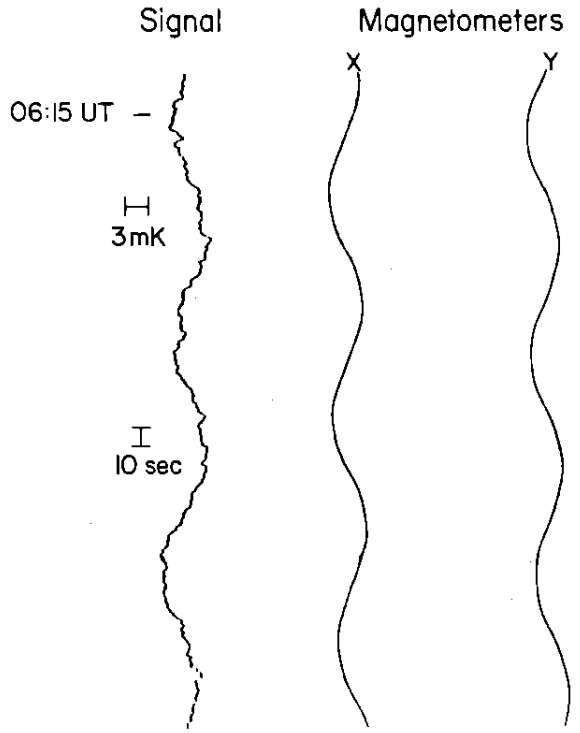

Fig. 3. - Section of telemetered data, April 1982 flight. Dipole is clearly evident.

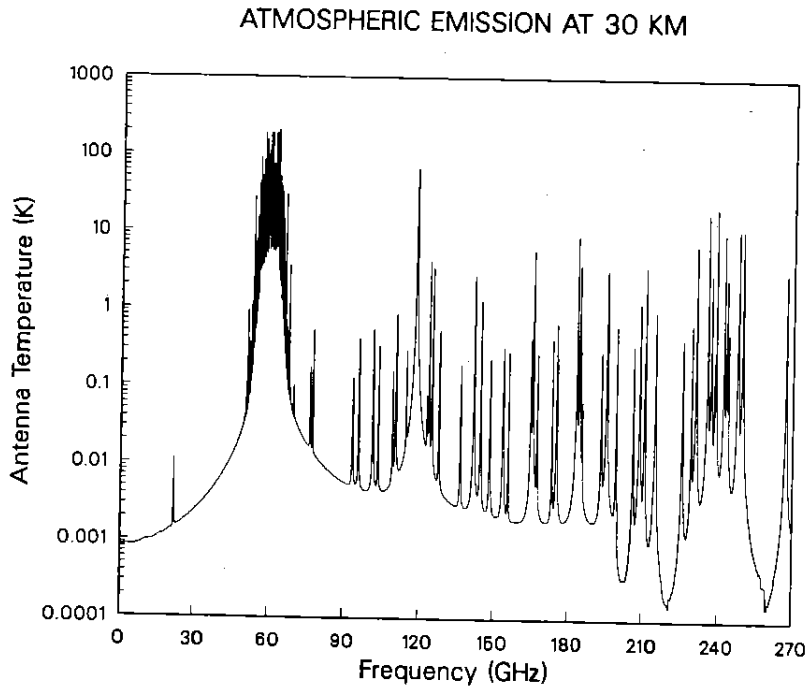

Fig. 4. - Calculated vertical atmospheric emission versus frequency. Radiometer passband is 88.3 to 91.7 GHz.

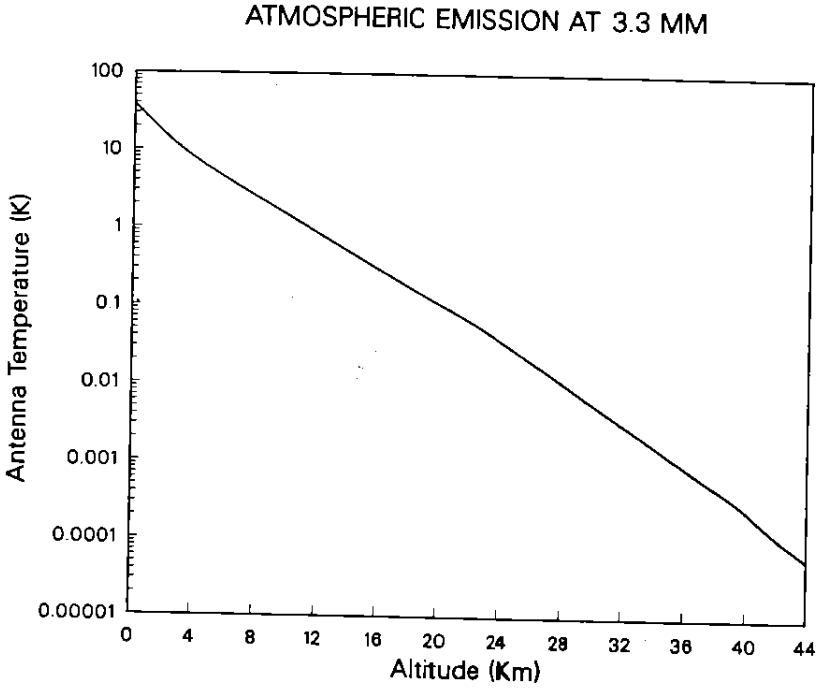

Fig. 5. - Calculated vertical atmospheric emission versus altitude.

serious at our frequency.

6. - GALACTIC BACKGROUNDS

Of all the possible systematic errors, emission from our galaxy is the most troublesome as it cannot be corrected by better shielding, improved receiver design or by flying higher (at least for altitudes below 10^{18} Km, where balloons are not yet available). Galactic emission presents a fundamental source of error for large scale anisotropy measurements. Figure 6 shows the estimated galactic backgrounds as a function of wavelength based on low frequency ($\sim$ GHz) surveys for synchrotron and H-II emission and on the MIT (Owens, Muehlner and Weiss 1979) measurements of dust pinned by our 3mm dust result (Lubin, Epstein and Smoot 1983). More recent measurements (Halpern 1983) indicate that the dust spectrum may be somewhat flatter than this. From this it appears as though there is a minimum or "window" near 3 mm with typical emission off the galactic plane estimated to be 0.1 mK or less. Unfortunately, dust emission from the galaxy is not well understood particularly at the longer mm wavelengths. The IRAS 100 μ (Hauser *et al.* 1984) data will aid in our understanding but mm wavelength surveys will be needed for serious galactic dust modeling to be useful in anisotropy measurements. We will return to this later.

7. - SKY COVERAGE

The instrument has been flown four times. The first flight was on July 1, 1981, from Palestine, Texas ($\delta = +31.8^\circ$). For the first flight the instrument was flown on the Princeton gondola (Wilkinson). Because of severe telemetry interference no useful data was obtained. The second flight, on November 4, 1981, also from Palestine, was on the M.I.T. gondola (Weiss). The third flight, on April 26, 1982, from Palestine, used our own gondola. The fourth flight, on November 19,

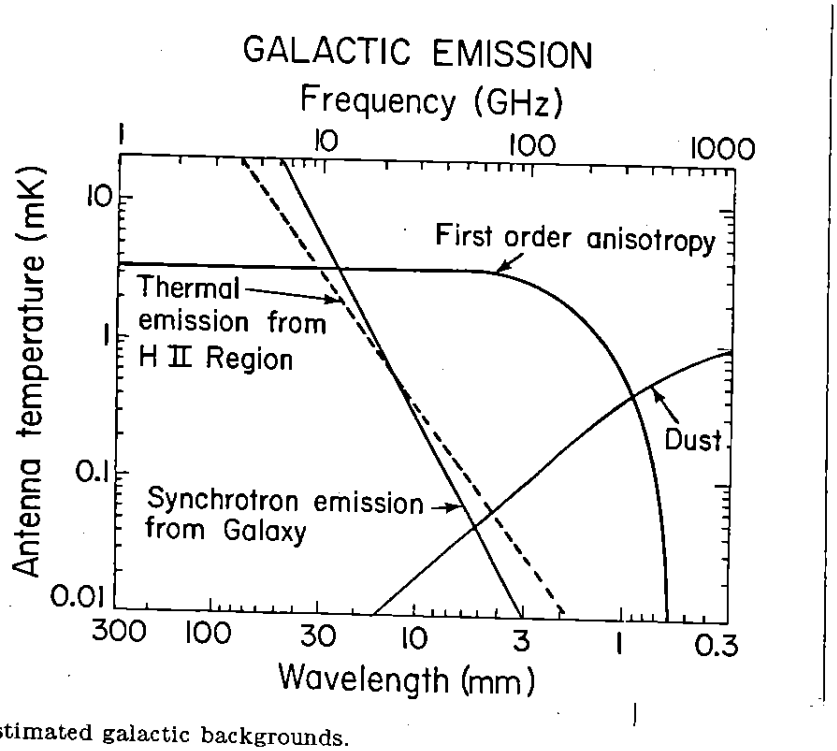

Fig. 6. - Estimated galactic backgrounds.

1982 used our gondola and was from Cachoeira Paulista, SP, Brazil (δ=-22.7°). Due to difficulties with the termination system, the gondola was not recovered though the data was recovered from the telemetry tapes. The sky coverage obtained from the three successful data flights is shown in Figure 7. Total sky coverage is 85%.

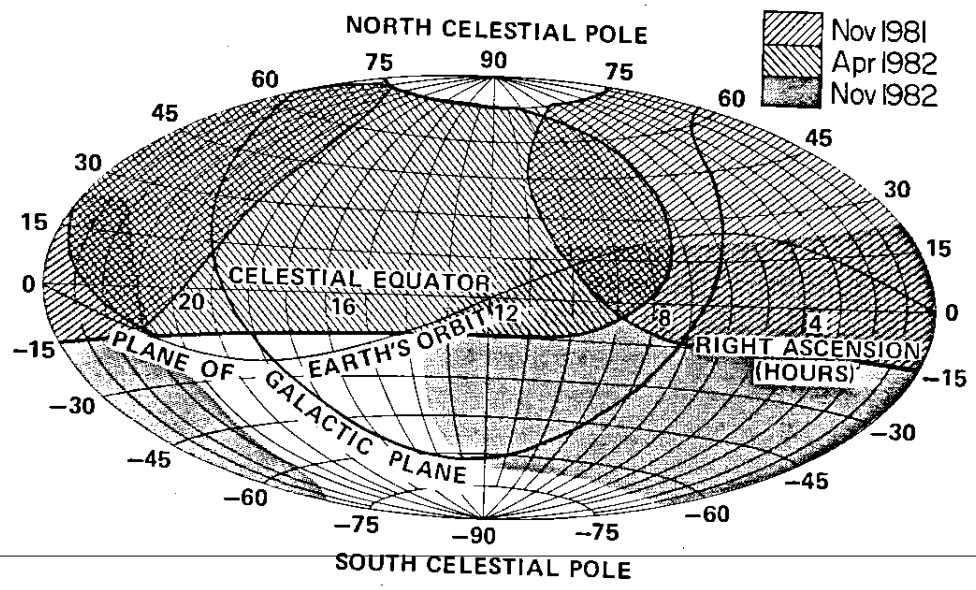

Fig. 7. - Sky coverage of flights as a Hammer-Aitoff projection. Total sky coverage is 85%.

8. - CALIBRATION

The instrument was calibrated before, during and after each flight, except for the last flight where no post-flight calibration was possible. Pre-flight and post-flight calibration consisted of using an ambient and liquid nitrogen target to establish the system gain. The system was carefully checked for saturation effects and a slight correction was made. The system was in flight configuration (cryogens in place and pressurized) during these calibration. Over a year's time interval the system gain for pre and post-flight calibration was within ± 1.5%. The first three flights used a small (~ 1% beam filling factor) blackbody target as an inflight calibrator. Calibration was performed every 27 minutes during the flight. While this small calibrator provided very good relative calibration, it was difficult to use as an absolute calibrator to better than 5%. For the last flight, it was replaced by a full beam target and appeared to be capable of a 1-2% calibration. Unfortunately, as the flight recorder data tape was not recovered this full accuracy has not been achieved. However, during the last flight, the moon was directly viewed and was also used as a calibration source. Calculations of the full beam equivalent brightness temperature at 3.3 mm of the moon due to Kelhm (1984) are shown in Figure 8. For this flight, the phase of the moon was - 134°. The moon calibration agrees within 2% of that obtained with the target calibrator. The relative gain stability during all the flights was ± 1%. One number is found to be sufficient to use as a calibration constant for all flights. Overall, we place a calibration error of 5% on the data.

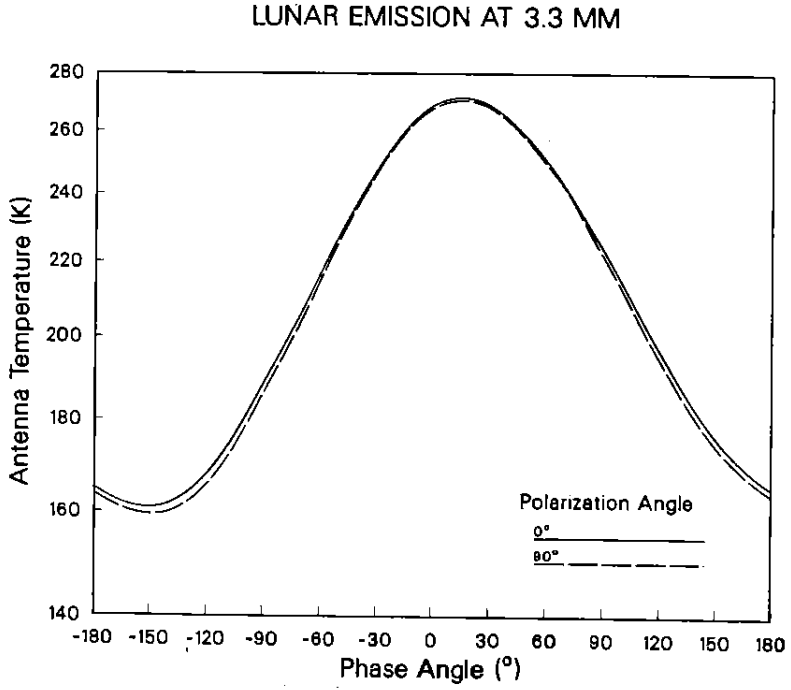

Fig. 8. - Full disk equivalent brightness temperature of the moon versus phase angle. Phase angle for the Brazilian flight was -134°.

9. - DATA ANALYSIS

After removal of the offset and calibration, the data is fit to a series of functions using a least-square fitting algorithm A summary of dipole and quadrupole spherical harmonic fits is given in Table I. As can be seen, no significant

quadrupole remains. The dipole amplitude errors are dominated by the 5% calibration error. The dipole direction is $\alpha = 11.3 \pm 0.1$ hours and $\delta = -6.0 \pm 1.4$ degrees in celestial coordinates. Because of the relative calibration stability and magnetometer pointing reconstruction (better than 1° from the moon data) the accuracy of the dipole direction is not limited by the 5% amplitude calibration error but is good to about 2%. The quadrupole fits imply a 90% confidence level upper limit of 7×10^{-5} on an RMS quadrupole component.

TABLE I

SPHERICAL HARMONICS FITS					
FIT	COEFFICIENTS	ALL DATA	GALACTIC CUT 5°	STATISTICAL ERROR	TOTAL ERROR
Dipole	T_x	-2.73	-2.73	0.06	0.14
	T_y	0.50	0.58	0.06	0.08
	T_z	-0.30	-0.29	0.05	0.08
Dipole and Quadrupole	T_x	-2.74	-2.74	0.07	0.14
	T_y	0.51	0.56	0.07	0.08
	T_z	-0.40	-0.34	0.07	0.08
	Q_1	0.17	0.08	0.07	0.08
	Q_2	0.22	0.12	0.07	0.08
	Q_3	0.13	0.10	0.08	0.09
	Q_4	-0.08	-0.07	0.06	0.07
	Q_5	0.04	0.07	0.05	0.07

Values are mK antenna temperature mult. by 1.23 to convert to thermodynamic temperature for T=2.7 K, see Table III.

$T = T_x\cos\delta\cos\alpha + T_y\cos\delta\sin\alpha + T_z\sin\delta + Q_1(3\sin^2\delta - 1)/2 + Q_2\sin2\delta\cos\alpha + Q_3\sin2\delta\sin\alpha + Q_4\cos^2\delta\cos2\alpha + + Q_5\cos^2\delta\sin2\alpha$

Table I - Dipole and Quadrupole fits to 3 mm data. Galactic cut 5° is fit excluding data within 5° of the galactic plane. Total error includes 5% calibration error.

10. - ORBITAL VELOCITY

The velocity of the earth about the sun is approximately 30 Km/sec or 10^{-4} c. The velocity of the earth relative to the cosmic background radiation is approximately 10^{-3} c. Dipole measurements taken 6 months apart should be able to resolve the earth's orbital motion as a 10% effect on the dipole. For the April 1982 and November 1982 flights the measured difference in velocity vectors (dipoles) between the flights is

$$(\Delta T_X\ ,\ \Delta T_Y\ ,\ \Delta T_Z) = (-0.30\pm0.14,\ 0.40\pm0.14,\ 0.08\pm0.14)\ ,$$

where the numbers are antenna temperature in mK. The predicted difference based on the earth's orbital parameters is (-0.32, 0.28, 0.12) in good agreement. For these two flights the orbital effect is not just a change in dipole amplitude but both an amplitude and direction shift. Detection of the earth's orbital motion is a good cross check of subtle systematic errors, especially relative pointing and calibration errors.

11. - GALACTIC EMISSION

Inclusion or exclusion of the galactic plane has very little effect on the fits, changing the dipole and quadrupole parameters by less than 0.1 mK. Galactic emission appears to be a small effect in this data. A fit to a cosec b (galactic latitude) dust model, flattened at b = 5°, yields 41 ± 11 μK at the poles. While this appears to be significant, it should be interpreted cautiously. Excluding data within 5° of the galactic plane and repeating the fit gives an insignificant 14 ± 19 μK as the pole value. Interpreting this fit as being indicative of galactic emission at 3 mm, we can combine this data with other recent centimeter, millimeter and submillimeter data. The result is shown in Figure 9.

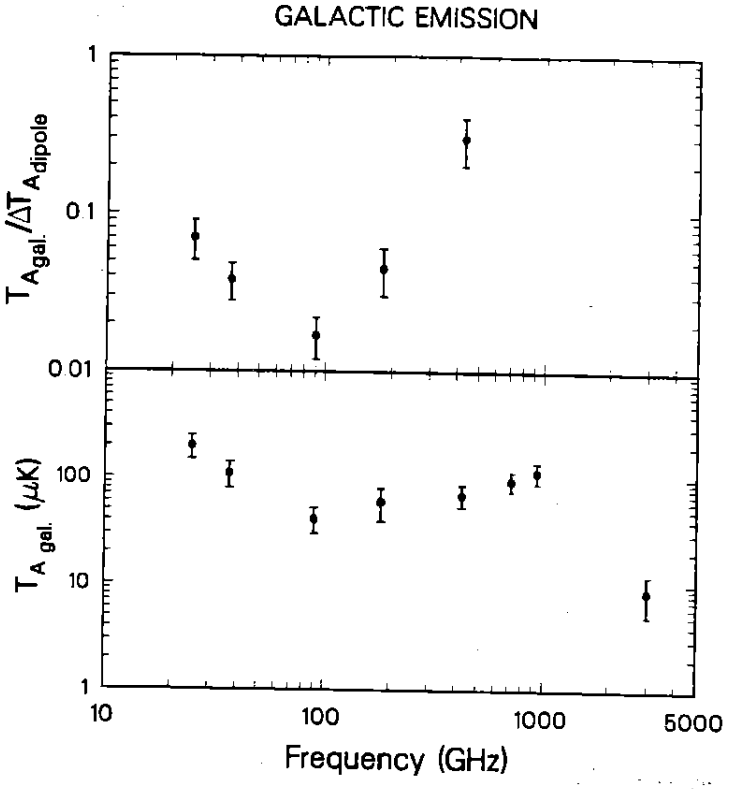

Fig. 9. - Recent measurements of large scale galactic emission. Lower data is fit to galactic model (cosec (b) or similar) in antenna temperature. Upper data is the ratio of galactic model fit to dipole at the frequency for T = 2.7 K. Data: 1) 3000 GHz point is IRAS 100 μ data, Hauser *et al.* (1984), 2) 100 to 1000 GHz points are Halpern *et al.* (1984), 3) 90 GHz is this work, 4) 37 GHz is Strukov *et al.* (1984) and 5) 25 GHz is Fixsen (1982).

12. - MAPS

To convert the approximately 10^5 measurements of temperature differences to a map of the sky requires some manipulation of the data. The general idea is to find a temperature distribution (map) T_i which minimizes the χ^2 of the map compared to the actual difference data. Minimizing

$$\chi^2 = \sum \frac{1}{{\sigma_{ij}}^2} (T_i - T_j - \Delta T_{ij})^2 \ ,$$

where T_i and T_j are the desired map temperatures at pixels i and j and ΔT_{ij} is the measured temperature difference between pixels i and j. For this the T_i are considered free parameters. Minimizing the χ^2 with respect to T_i yields a set of N linear equations where N is the number of pixel elements. These equations take the form:

$$\sum_{1}^{N} \frac{1}{\sigma_{ij}^{\,2}} (T_i - T_j - \Delta T_{ij}) = 0 \quad .$$

Our antenna has a nearly gaussian beam profile with a 7° full width at 3 dB (half power point). The integrated beam pattern is about 70 square degrees. This gives about 600 independent sky patches for the full sky. We split each patch into 4 parts giving about 2400 pixels on the full sky or 2000 pixels for our 85% sky coverage. Solving the 2000 linear equations is tantamount to inverting a 2000 x 2000 sparse matrix. Instead of a direct matrix inversion, we use an iterative Gauss-Sidel inversion technique (Gulkis and Janssen 1981) which is efficient at inverting large matrices. The method converges rapidly, typically within 100 iterations. As a subsidiary condition, the weighted map average is set equal to 0, since the absolute temperature is not determined.

A map made using this technique is given in Figure 10 as a $\sin\delta$ projection, which is an equal area projection. The map clearly shows the dipole. A residual map after the dipole is removed is shown in Figure 11. The large scale features of the data are faithfully reproduced in the sense that a fit of the map to dipole and quadrupole harmonics gives (within errors) the same values as fitting the (differential) data. Because the data is taken at essentially constant latitude the matrix is nearly singular and certain subtle mathematical instabilities can occur. To test the stability of our maps, a number of Monte Carlo simulations were run. They show that on large scales the map is a faithful reproduction of the data.

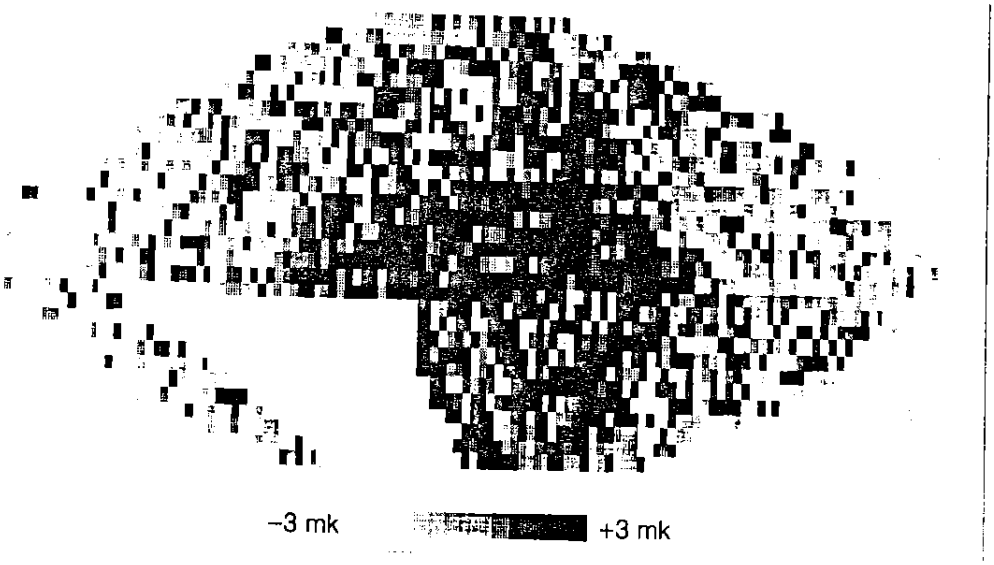

Fig. 10. - 3 mm map as a $\sin\delta$ projection in celestial coordinates (α,δ). $\alpha = +24$ hr. at left and 0 hr. at right. $\delta = +77°$ at top and -68° at bottom. Sky coverage is 85%. Pixels are nominal 3° x 5° (α x δ).

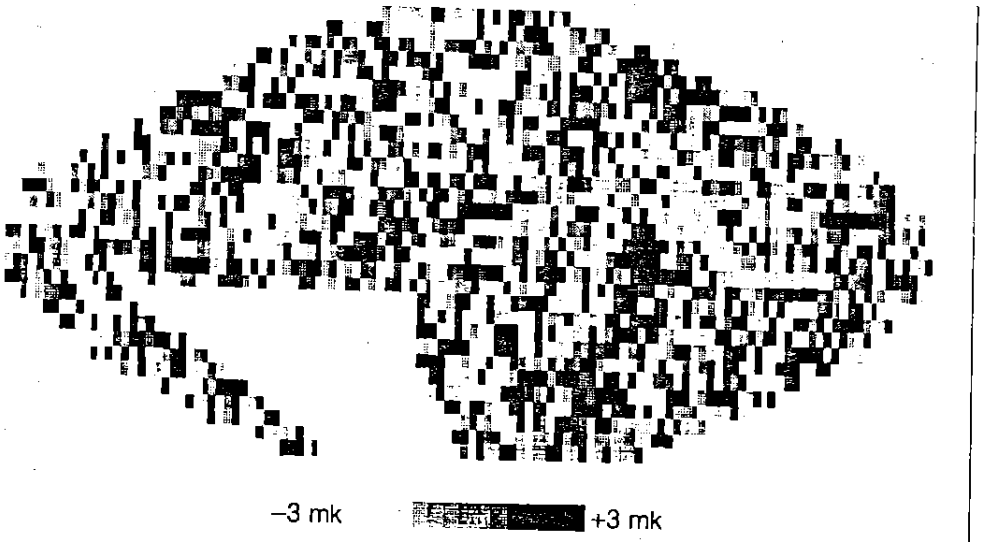

Fig. 11. - Residual map after subtraction of dipole. Parameters the same as figure 10.

13. - COMPARISON TO OTHER DATA

The dipole has been measured from 1 mm to 3 cm by various groups using both broadband incoherent (bolometer) techniques for $\lambda < 3$ mm and narrow band ($B \sim 1$ GHz) coherent (heterodyne) techniques for $\lambda > 3$ mm. Table II summarizes the dipole measurements.

TABLE II

RECENT DIPOLE MEASUREMENTS

Group	λ (mm)	Technique	Platform	Residual Atmosphere	Sky Coverage	Statistical Error	Calibration Error	Inflight Calibration	ΔT^* (mK)	ΔT_A (mK)
Berkeley [1]	9	M	U-2 (20 Km)	40 mK	60%	10%	5%	No	3.1 ± 0.4	3.0 ± 0.4
Berkeley [2]	3	M	Balloon (30 Km)	10 mK	85%	2%	5%	Yes	3.4 ± 0.2	2.8 ± 0.1
Florence [3]	0.5 - 3	B	Balloon (40 Km)	~ 1 K	10%	-	~ 20%	No	$2.9^{+1.6}_{-0.6}$	—
M.I.T. [4]	0.2 - 3	B	Balloon (40 Km)	0.2 K	50%	10%	~ 20%	Yes	3.0 ± 0.4	1.3 ± 0.2
Princeton [5]	7, 10, 12	M	Balloon (25 Km)	30 mK	50%	10%	5%	No	3.8 ± 0.3	3.7 ± 0.3
Princeton [6]	12	M	Balloon (25 Km)	20 mK	80%	1%	5%	Yes	3.1 ± 0.2	3.0 ± 0.2
Moscow [7]	8	M	Satellite	0 mK	100%	?	?	Yes	2.4 ± 0.5	—

M — Microwave (coherent) B — Bolometer (incoherent)

*Assuming CBR is blackbody and T = 2.7K.

[1]Smoot and Lubin 1979; inflight calibration by moon in some flights, noise diode calibrator in last few flights. Sky coverage in patches.

[2]Lubin, Epstein and Smoot 1983; Epstein 1983; This work.

[3]Fabbri, Guidi, Melchiorri and Natale 1980; no frequency resolution.

[4]Halpern 1983; 4 frequency bands (0.2-3mm), short wavelength bands to measure galactic dust, residual atmosphere for lowest frequency channel.

[5]Cheng 1983.

[6]Fixsen, Cheng and Wilkinson 1983; Fixsen 1982.

[7]Strukov and Skulachev 1984; Strukov, Sagdeev, Kardashev, Skulachev and Eysmont 1984; preliminary results.

Table II - Recent dipole measurements and experimental parameters.

The most accurate centimeter wavelength experiment is the Princeton 12 mm maser experiment. With comparable sky coverage and sensitivity, a fruitful comparison can be made. This is shown in Table III. As can be seen, the two data sets are in good agreement for the quadrupole parameter limits. The dipole directions are virtually identical (within 3°). The dipole amplitudes are compared below.

TABLE III

COMPARISON BETWEEN 3 MM AND 12 MM FITS
Values in thermodynamic temperature for T=2.7 K

COEFFICIENTS	3 MM[1] DATA	12 MM[2] DATA
T_x	-3.35 ± 0.17	-3.01 ± 0.17
T_y	0.71 ± 0.10	0.56 ± 0.09
T_z	-0.35 ± 0.08	-0.28 ± 0.09
T_x	-3.37 ± 0.17	-3.07 ± 0.17
T_y	0.69 ± 0.09	0.67 ± 0.09
T_z	-0.42 ± 0.09	-0.45 ± 0.09
Q_1	0.10 ± 0.09	0.15 ± 0.08
Q_2	0.15 ± 0.10	0.15 ± 0.11
Q_3	0.12 ± 0.11	0.14 ± 0.07
Q_4	-0.09 ± 0.09	0.06 ± 0.11
Q_5	0.08 ± 0.08	-0.01 ± 0.07

[1] *Excludes data within 5° of the galactic plane.*
[2] *Fixsen, Cheng and Wilkinson (1983).*
Errors include calibration.

Table III - Comparison of 3 mm (this work) with 12 mm (Fixsen 1982) results. Errors include calibration errors. The values are in thermodynamic temperatures, assuming a T = 2.7 K blackbody.

14. - DIPOLE COMPARISON

As discussed before, comparing measurements of the dipole at different wavelengths can yield information about the spectrum of the radiation. Figure 12 shows the amplitude of various dipole measurements. As can be seen even at similar wavelengths, there is some disagreement. This may be partly due to the lack of inflight calibration, for some early measurements, as well as the lack of good sky coverage. Calibration is a severe problem for the broadband bolometer experiments, where even ground calibration is difficult. These problems will limit the usefulness of this comparison.

Given a particular spectrum $T_A(\nu)$, we can test the hypothesis that the velocity vectors determined by two experiments are equal (i.e. that they are measuring the same physical effect) or that the difference in velocity vectors is zero. It can be shown that

$$S = \vec{d}^{\,T}\, \mathbf{E}^{-1}\, \vec{d}\ ,$$

where

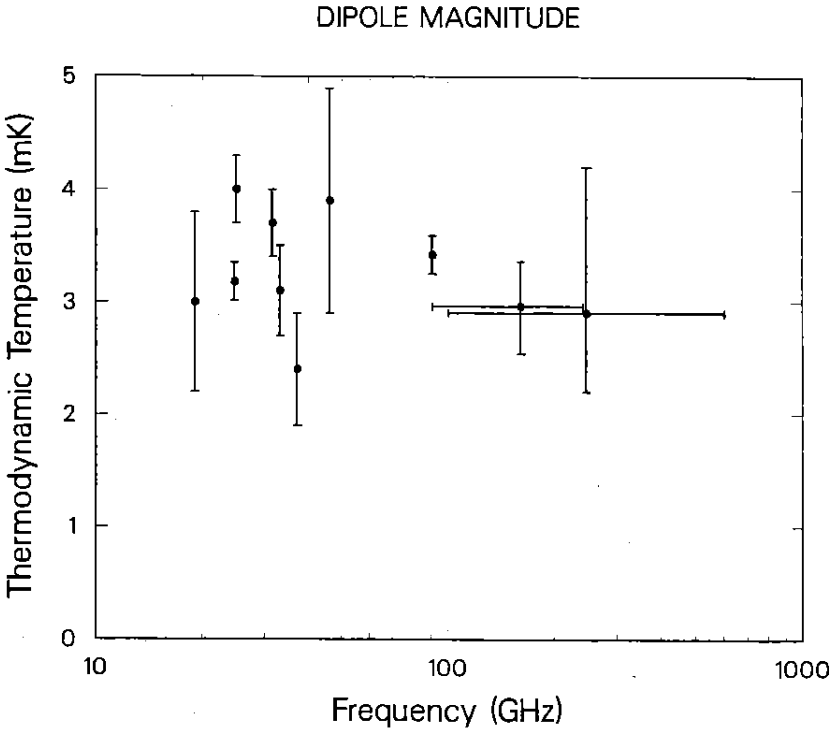

Fig. 12. - Recent dipole measurements. This work at 90 GHz. Other data are Boughn, Cheng and Wilkinson (1981); Smoot and Lubin (1979); Fixsen, Cheng and Wilkinson (1983); Halpern (1983) and Fabbri *et al.* (1980).

$$\vec{d} = \vec{\beta}_1 - \vec{\beta}_2 \quad \text{and} \quad \mathbf{E} = \mathbf{E}_1 + \mathbf{E}_2$$

is distributed like a chi square with 3 degrees of freedom (Martin 1971; Gorenstein 1978). Here $\vec{\beta}_1$, and $\vec{\beta}_2$ are the two measured velocity vectors and $\mathbf{E}_1$ and $\mathbf{E}_2$ are the associated error matrices. Given a spectrum $T_A(\nu)$, the spectral index $\alpha(\nu)$ can be determined. From $T_A(\nu)$ and $\alpha(\nu)$ the velocity vector $\vec{\beta}$ can be inferred from the measured dipole $\Delta\vec{T}_A$ using:

$$\Delta\vec{T}_A = T_A\,(3-\alpha)\vec{\beta} \ .$$

With the velocity vector $\vec{\beta}$ the above test can be performed. Using the Princeton 12 mm data to compare our data to is summarized in Table IV. The test indicates a general agreement with a 2.7 K blackbody but is inconclusive with regard to the Woody and Richards data (Lubin *et al.* 1984).

15. - FUTURE

Anisotropy measurements have increased in sensitivity by about three orders of magnitude since they were started nearly twenty years ago. The major emphasis has been on improving the sensitivity of the instruments since this was the limiting factor. Now, particularly for the very large scale ($\theta > 30^\circ$) measurements, galactic emission is becoming a serious source of error. Currently the uncertainty in the first few spherical harmonic terms is about 100 μK. Reducing this by another order of magnitude will be difficult regardless of the system sensitivity unless fundamental advances are made in our understanding of galactic emission. Multiple frequency measurements are critical for this. Accurate absolute calibration will also be needed at about the 1% level to fully exploit the data

TABLE IV

COMPARISON BETWEEN 12 MM AND 3 MM DIPOLES

	12 mm[1]					3 mm[2]				
	FIT* (mK)	ERROR (mK)	CORRELATION COEFFICIENTS†			FIT* (mK)	ERROR (mK)	CORRELATION COEFFICIENTS†		
T_x	-2.96	0.17	1	0.11	0.11	T_x	-2.72	0.14	1	0.10	-0.04
T_y	0.55	0.09		1	0.18	T_y	0.51	0.08		1	-0.12
T_z	-0.28	0.09			1	T_z	-0.33	0.08			1

Spectrum	Confidence Level
2.7 K	35%
3.0 K	65%
2.7 K @ 12mm, W − R @ 3mm††	3%
3.0 K @ 12mm, W − R @ 3mm††	49%

*measured antenna temperature.

†correlation coefficient $c_{ij} = \frac{\epsilon_{ij}}{\sqrt{\epsilon_{ii}\epsilon_{ij}}}$, ϵ_{ij} error matrix $\sqrt{\epsilon_{ii}}$ = error in T_i or β_i.

†† W − R fit to data of Woody and Richards 1979 see text.

[1]Fixsen, Cheng and Wilkinson, 1983.

[2]This work; includes cosec b fit to galaxy.

Table IV - Consistency of 12 mm and 3 mm dipoles as a test of different spectra.

when comparing different measurements. Relative calibration stability will also be very important for long term satellite measurements and widely spaced balloon flights.

New technologies such as superconducting (SIS) receivers and ^{3}He bolometer systems as well as older technologies such as masers, promise near order of magnitude increases in system sensitivity within the next few years with the resultant decrease in observing time for background limited measurements from months to days or less. Satellite observations are already underway with the Prognos 9 (Strukov *et al.* 1984) mission recently completed and the COBE (Cosmic Background Explorer) satellite due to be launched later this decade. Within five years a variety of background limited measurements at different frequencies should be available.

This work was supported by the California Space Institute under CS 48-81, by the National Aeronautics and Space Administration under NAGW-66, by the National Science Foundation under SPI 8166057 and by the U.S. Department of Energy under DE-AC03-76SF00098. The northern hemisphere balloon launches were conducted by NASA at the National Scientific Balloon Facility, Palestine, Texas. The southern hemisphere flight was also supported by the Instituto de Pesquisas Espaciais/CNPq. One of us (T.V.) is supported by Conselho Nacional de Desenvolvimento Científico e Tecnológico (CNPq) under 202372/83-FA and Fundação de Amparo à Pesquisa do Estado de São Paulo (FAPESP) under 83/9834-1-Astronomia. We gratefully acknowledge the previous contributions to this work made by G. Epstein and G. Smoot. This work is a continuation of Lubin, Epstein and Smoot (1983). This project would not have been fruitful without the encouragement and assistance of D. Wilkinson on whose gondola we flew for the first time. We appreciate the perseverance of the MIT group and especially of R. Weiss in allowing us to fly our "MIT/Bezerkeley Lunar Lander". Special thanks go to P. Price, N. Boggess, R. Kubara, and the staff of the National Scientific Balloon Facility for their assistance and hospitality. The southern hemisphere flight was made possible by the generous assistance and cooperation of the Instituto de Pesquisas Espaciais (INPE) and in particular with the support of N. Parada. O trabalho e dedicação de todo o pessoal do Departamento de Astrofísica do INPE, e particularmente o incentivo e apoio recebidos por parte de J. Braga, R. Corrêa e U. Jayanthi, foram imprescindíveis e colaboraram de forma decisiva na realização deste trabalho. We note in passing the heroic efforts of J. Flambard, A. Spurlock and V. Kelly in helping to prepare this paper. This experiment was stimulated by the work of Smoot, Gorenstein and Muller (1977) and Muller (1978).

REFERENCES

Boughn,S., Cheng,E., and Wilkinson,D.T. 1981, *Astrophys. J. Lett.*, **243**, L113.
Cheng,E. 1983, *Ph.D. Thesis*, Princeton University.
Compton,A., and Getting,I. 1935, *Phys. Rev. Lett.* **47**, 817.
Cong,H., Kerr,A.R., and Mattauch,R.J. 1979, *IEEE TMTT* **27**, 3, 245.
Danese,L., and De Zotti,G. 1981, *Astron. Astrophys.* **94**, L33.
de Bernardis,P., Masi,S., Melchiorri,F., and Moleti,A. 1984, *Astrophys. J. Lett.* **284**, L21.
Epstein,G.L. 1983, *Ph.D. Thesis*, University of California, Berkeley.
Fabbri,R., Guidi,I., Melchiorri,F., and Natale,V. 1980, *Phys. Rev. Lett.* **44**, 1563.
Fixsen,D.J. 1982, *Ph.D. Thesis*, Princeton University.
Fixsen,D.J., Cheng,E.S., and Wilkinson,D.T. 1983, *Phys. Rev. Lett.* **50**, 620.
Georgi,H., Ginsparg,P., and Glashow,S.L. 1983, *Nature* **306**, 765.
Gorenstein,M.V. 1978, *Ph.D. Thesis*, University of California, Berkeley.
Gulkis,S., and Janssen,M. 1981, *NASA COBE report no.* **4004**.
Halpern,M. 1983, *Ph.D. Thesis*, Massachusetts Institute of Technology.
Halpern,M., Wright,E., Weiss,R., and Benford,R. 1984, *preprint.*
Hauser,M.G., Gillett,F.C., Low,F.J., Gautier,T.N., Beichman,C.A., Neugebauer,G., Aumann,H.H., Baud,B., Boggess,N., Emerson,J.P., Houck,J.R., Soifer,B.T., and Walker,R.G. 1984, *Astrophys. J. Lett.* **278**, L15.
Keihm,S. 1984, *private communication* .
Lubin,P. 1980, *NASA COBE report no.* **5020**.
Lubin,P. 1982, paper in *Proceedings of the International School of Physics "Enrico Fermi", Course on Gamow Cosmology* ,Varenna.
Lubin,P., Epstein,G., and Smoot,G. 1983, *Phys. Rev. Lett.* **50**, 616.
Lubin,P., Fixsen,D., Cheng,E., and Epstein,G. 1984, *submitted to Astrophys. J.*.
Martin,B. 1971, *Statistics for Physicists*, Academic Press.
Muller,R. 1978, *Scientific American* **238**, 5, 64.
Owens,D.K., Muehlner,D.J., and Weiss,R. 1979, *Astrophys. J.* **231**, 702.
Smoot,G., and Lubin,P. 1979, *Astrophys J. Lett.* **234**, L83.
Smoot,G., Gorenstein,M., and Muller,R. 1977, *Phys. Rev. Lett.* **39**, 898.
Strukov,I.A., and Skulachev,D.P. 1984, *Sov. Astron. Lett.* **10** , 1.
Strukov,I.,Sagdeev,R.,Kardashev,N.,Skulachev,D.,and Eysmont,N. 1984, *preprint.*
Uson,J.M., and Wilkinson,D.T. 1984, *preprint.*
Woody,D., and Richards,P. 1979, *Phys. Rev. Lett.* **42**, 925.